

Electrospinning of Ionic Supramolecular Azo Complexes

Xiaoxiao Wang, Qian Zhang, C. Geraldine Bazuin,* Christian Pellerin*

Summary: Electrospinning was applied to DMF solution mixtures of poly(methyl methacrylate) (PMMA) and MO/PVP, which is an azo-containing liquid crystalline complex between methyl orange (MO) and methylated poly(4-vinyl pyridine) (PVP), to obtain composite light-responsive fibers. The average diameter of the fibers, which ranged from 700 nm to 1.5 μm , increases with PMMA content. Differential scanning calorimetry, X-ray diffraction and transmission electron microscopy show that they are microphase separated in the form of interspersed nanostrips of PMMA-rich and MO/PVP(-rich) phases. The MO/PVP(-rich) phase is liquid crystalline (smectic A) as in the bulk, but with no orientation relative to the fiber axis. The birefringence of the fibers observed by polarized optical microscopy is attributed, at least in part, to form birefringence. This study is promising for the preparation of light-responsive fibers based on easy-to-prepare polymer complexes.

Keywords: azobenzene; electrospinning; ionic complexation; liquid crystalline complex; polymer complex

Introduction

Electrospinning is a widely used technique for preparing nanofibers with promising applications in nanotechnology and life sciences due to their large surface/mass ratio.^[1] The fibers are obtained by applying a high electric field to a polymer solution causing the ejection of a charged jet that rapidly dries while being subjected to a whipping motion. In order to collect continuous fibers rather than electro-sprayed droplets, the viscosity of the solution must be sufficiently high to prevent breakup of the jet by Rayleigh instabilities. Electrospinning has therefore been mostly applied to concentrated solutions of polymers, polymer blends, and composites that have sufficiently flexibility and high molecular weight to create a well-entangled network in solution.^[2–4] In the last few years, our group has shown that hydrogen-

bonded supramolecular complexes between a polymer, such as poly(ethylene oxide) (PEO), and small molecules can readily be electrospun.^[5,6] Efficient complexation and crystallization was observed for systems forming intercalates and inclusion complexes, even if the solvent evaporation occurs on a millisecond time scale. The electrospinning of inclusion complexes of polymers with cyclodextrin and of clathrates of syndiotactic polystyrene has also been demonstrated recently.^[7,8]

Polymers with an extended structure in solution, in particular polyelectrolytes, form a less developed entanglement network in solution and are therefore much harder to electrospin.^[9] They nevertheless present very interesting attributes such as the possibility of functionalization through ionic interactions with various charged small molecules that act as supramolecular side-chains. Azobenzene (or azo for short) molecules are well known for their efficient photoisomerization process^[10] that allows controlling molecular orientation with polarized laser light.^[11] Recently, a light-driven motor was developed by the Ikeda

Département de chimie and Centre for Self-Assembled Chemical Structures, Université de Montréal, Montréal, QC, H3C 3J7, Canada
E-mail: geraldine.bazuin@umontreal.ca;
c.pellerin@umontreal.ca

group based on light-induced reorientation in laminated films of azo-containing liquid-crystalline elastomers,^[12] revealing their potential as artificial muscles.^[13] Some of us have shown that efficient ionic complexation is possible between methyl orange (MO) and methylated poly(4-vinylpyridine) (PVP) (Figure 1). This complex leads to materials that possess high glass transition ($T_g = 183^\circ\text{C}$) and degradation ($T_d^{1\%} = 222^\circ\text{C}$) temperatures.^[14] It was shown to form a smectic A liquid crystalline phase despite the absence of a flexible spacer or tail group in MO. This structure enabled the generation of high and stable photoinduced orientation and the efficient fabrication of surface relief gratings.^[14,15] Azo-containing liquid crystalline polymers such as the MO/PVP complex may therefore be good candidates for producing photoaddressable nanofibers. In fact, light-induced shrinkage of azo-containing nylon and acetate fibers, although only on the order of 0.1%, has been observed as early as 1966.^[16] Such low shrinkage was attributed to the fabric thickness (6 cm) that limited light penetration and to the low content of loosely bound dye. It is expected that the photo-mechanical effect may be improved using a higher load of strongly bound azo in nanofibers.

However, the electrospinning of liquid crystalline polymers is challenging for the same reason as polyelectrolytes; that is, due to their extended chain conformation in solution that prevents the formation of a well-entangled network.^[17] A few groups have successfully prepared electrospun fibers from main-chain LC polymers.^[18,19] In contrast, side-chain LC polymers have only been electrospun successfully when blended with PEO because of their even

higher rigidity due to the stacking and steric hindrance of the side groups.^[20] In this work, we show that fibers of the MO/PVP complex can be successfully prepared when mixed with poly(methyl methacrylate) (PMMA), despite having both polyelectrolyte and liquid crystalline character. This thus represents an initial step towards the fabrication of nanofibers of side-chain liquid crystalline photoresponsive polyelectrolyte complexes.

Experimental Part

Materials

Poly(methyl methacrylate) (PMMA) ($M_w = 540\text{K}$) and poly(4-vinyl pyridine) (PVP) ($M_v = 200\text{K}$) from Scientific Polymer Products, methyl orange (MO), iodomethane (99.5%), nitromethane (95 + %) and dimethylsulfoxide (DMSO, 99.9%, spectrophotometric grade) from Aldrich and diethyl ether and anhydrous dimethyl formamide (DMF) (99.8%) from EMD were all used as received. Deionized water was obtained from a Millipore Gradient A10 Milli-Q system (resistivity $18.2\text{ M}\Omega\cdot\text{cm}$ at 25°C). The stoichiometric MO/PVP complex was prepared according to the procedures described elsewhere.^[14,15] Briefly, 1 eq. of PVP was first fully methylated by stirring with iodomethane (5 eq.) in nitromethane at 45°C for 5 days. The precipitated methylated PVP was dissolved in water and then reprecipitated from diethyl ether. Methylated PVP and MO (with a 14% molar excess) were dissolved separately in DMSO, then mixed together, and finally dialyzed against deionized water for a few days. The 1:1 MO:VP molar ratio in the final product was confirmed by NMR and elemental analysis. The chemical structures

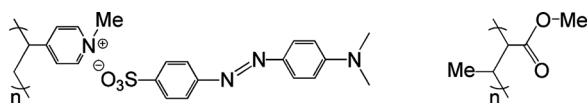


Figure 1.

Molecular structure of (left) the complex between methyl orange (MO) and methylated poly(4-vinyl pyridine) (PVP) and (right) poly(methyl methacrylate) (PMMA).

of the MO/PVP ionic complex and of PMMA are shown in Figure 1.

Fiber Preparation

Solutions of PMMA and MO/PVP were prepared in DMF by warming with a heat gun to ca. 60 °C under stirring (Vortex mixer, Fisher Scientific) to form transparent solutions with a total solid content of 15 wt % (unless otherwise specified). In addition to the pure PMMA and pure MO/PVP, solutions were prepared with 1:2, 1:1 and 2:1 PMMA:MO/PVP weight ratios (abbreviated as MMA/MO 1/2, MMA/MO 1/1 and MMA/MO 2/1, respectively). Each solution was transferred to a glass syringe, mounted on a syringe pump (PHD 2000, Harvard Apparatus), and extruded through a 0.41 mm needle at a rate of 0.008 mL/min. A +20 kV voltage was applied to the needle using an FC series 120 W regulated high voltage DC power supply (Glassman High Voltage). The collector consisted of parallel cylinder electrodes (diameter = 3.5 mm) separated by a gap of 2.7 cm, and connected to –2 kV cathode of a Nim Standard HV power supply (Power Design). The distance between the tip of the needle and the collector was 10 cm. The fibers were dried in a vacuum oven at 60 °C for 12 h.

Characterization

Polarizing optical microscopy (POM) micrographs were recorded using an Axioskop 40 microscope (Carl Zeiss) with a 20X objective. Scanning electron microscopy (SEM) was performed with a FEI Quanta 200 FEG environmental scanning electron microscope, for which the sample was first coated with gold (Sputter Coater, Agar Scientific). Differential scanning calorimetry (DSC) thermograms were obtained with a Q2000 calorimeter (TA Instruments) at a 10 °C/min scanning rate. Thermogravimetric analysis was done with a TGA 2950 from TA Instruments. X-ray diffraction (XRD) measurements were performed with a Bruker AXS D8 Discover system equipped with a 2D wire-grid detector, using the Cu K α radiation. Transmission electron microscopy (TEM)

micrographs were obtained with an FEI Tecnai 12 microscope working at 120 kV and equipped with a Gatan 792 Bioscan 1k x 1k wide angle multiscan CCD camera. To enhance the contrast, the fiber was immersed in a 0.1 wt % K₂Cr₂O₇ aqueous solution for 24 h, then in deionized water for 24 h, then freeze-dried and embedded in LR White (London Resin) and cured at 60 °C for 48 h. Finally, the sample was cut into thin slices with a microtome (Ultracut E, Reichert-Jung) equipped with Diatome knife.

Results and Discussion

The electrospinning of DMF solutions of the pure MO/PVP complex was attempted first, since it should lead to nanofibers with the largest photomechanical response. Unfortunately, electrospinning of these solutions at concentrations up to 50% only lead to electrosprayed droplets. At still higher concentrations, the solutions became too viscous to be electrospun. This is in line with the well-known difficulties in obtaining electrospun fibers of pure polyelectrolytes like chitosan,^[3] alginate,^[21] and Nafion,^[22] which is attributed to the repulsive forces between the charges along the backbone that cause chain extension and thereby inhibit the formation of entangled solutions.^[23] For the MO/PVP complex, the bulky MO side chains and the possible stacking of their aromatic rings further contribute to the chain rigidity in solution. The use of solvents that interact strongly with polyelectrolytes was suggested to facilitate fiber formation.^[3,21] However, the MO/PVP complex is insoluble in most solvents, and DMF was found to be the only suitable solvent for electrospinning of this material.

Poly(methyl methacrylate) (PMMA) of high molecular weight (M_w = 540K) was therefore blended with the MO/PVP complex to assist in fiber formation by its ready formation of an entanglement network. Electrospinning of pure PMMA has already been well studied.^[24,25] Bright orange fibers

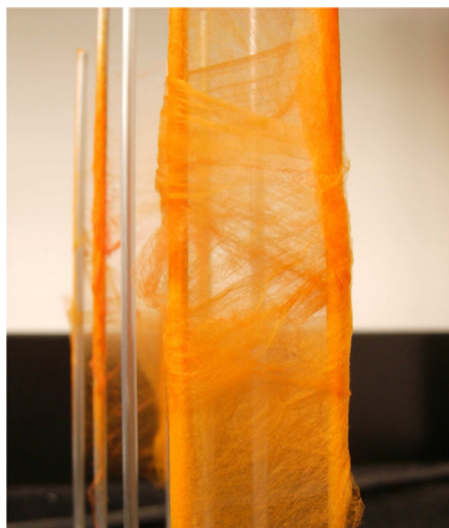


Figure 2.

Electrospun fibers (MMA/MO = 2/1) obtained on four pairs of collector. Some fibers are wrapped around the parallel rods (four collectors shown).

can be obtained in good yield when the MO/PVP complex is mixed with PMMA in 1:2, 1:1 or 2:1 weight ratios, as illustrated for a representative example in Figure 2. The fibers are mechanically stable over time and can be manipulated without obvious macroscopic damage. It should be mentioned here that PEO is used much more frequently than PMMA as an electrospinning matrix because its high tortuosity, due to the presence of an oxygen group in the main chain and the absence of any side group, allows chain entanglement and therefore electrospinning at much lower concentra-

tion. In fact, preliminary experiments indicated that electrospun fibers could also be obtained by adding PEO (1/1 weight ratio EO/MO) instead of PMMA; however, its use was not pursued because 1) its high degree of crystallinity leads to scattering that can disrupt light absorption by the MO chromophore and 2) its low melting point (65 °C) made the fibers mechanically unstable under the drying conditions used. In contrast, PMMA is an amorphous polymer with a high T_g and, given its excellent optical transparency, it should not interfere with light penetration in the fiber bundles.

Figure 3 shows cross-polarized optical micrographs of the electrospun fibers of MMA/MO mixed at different weight ratios with PMMA. The fibers do not show any bead defects, indicating that PMMA increases the viscosity of the solution sufficiently to prevent Rayleigh instability breakup of the electrospun jet. All fibers show a significant level of birefringence, as revealed by the intense color of segments aligned at $\pm 45^\circ$ relative to the polarizer direction and the complete extinction of those parallel to the polarizer and analyzer directions, as pointed out by arrows (observed clearly also by rotation of the sample between the crossed polarizers). The fibers are mainly orange or blue-green but it is difficult to interpret their color using the Michel-Levy scale because the effect of birefringence is convoluted with the visible absorption spectrum of methyl orange. The observation of birefringence is usually attributed to the presence of molecular

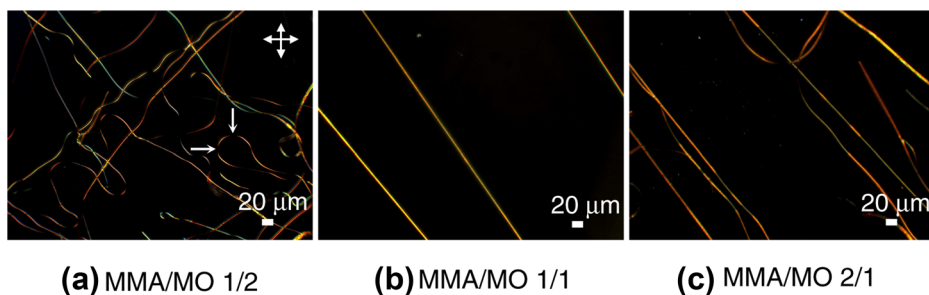


Figure 3.

Morphology and birefringence of the electrospun fibers as observed by polarizing optical microscopy. The arrows indicate the directions of the polarizer and analyzer.

orientation within the fibers, such as from the liquid crystalline domains and/or from polymer chains oriented relative to the fiber axis. This would be beneficial in the context of preparing light-responsive fibers, since the photomechanical effect should be larger for an initially oriented fiber than for an isotropic one. However, since the system contains phase separated components (see below) in an anisotropic material, the observations in Figure 3 can also be explained (at least in part) by “form birefringence”.^[26]

The fiber morphology was studied in more detail by scanning electron micro-

scopy. Figure 4 shows that the fibers have a smooth surface and that there are no ribbon- or dogbone-shaped fibers, suggesting that they are cylindrical. No beading defects were observed, although there were occasionally branching or sticking points as well as some breaks. Average diameters of fiber bundles were calculated by randomly sampling at least 100 fibers. Figure 5 indicates that the average diameter decreases from 1.5 μm to 700 nm as the MMA/MO weight ratio decreases from 2/1 to 1/2. The diameter distribution is also broader for fibers with a larger PMMA content. This trend can be explained by the

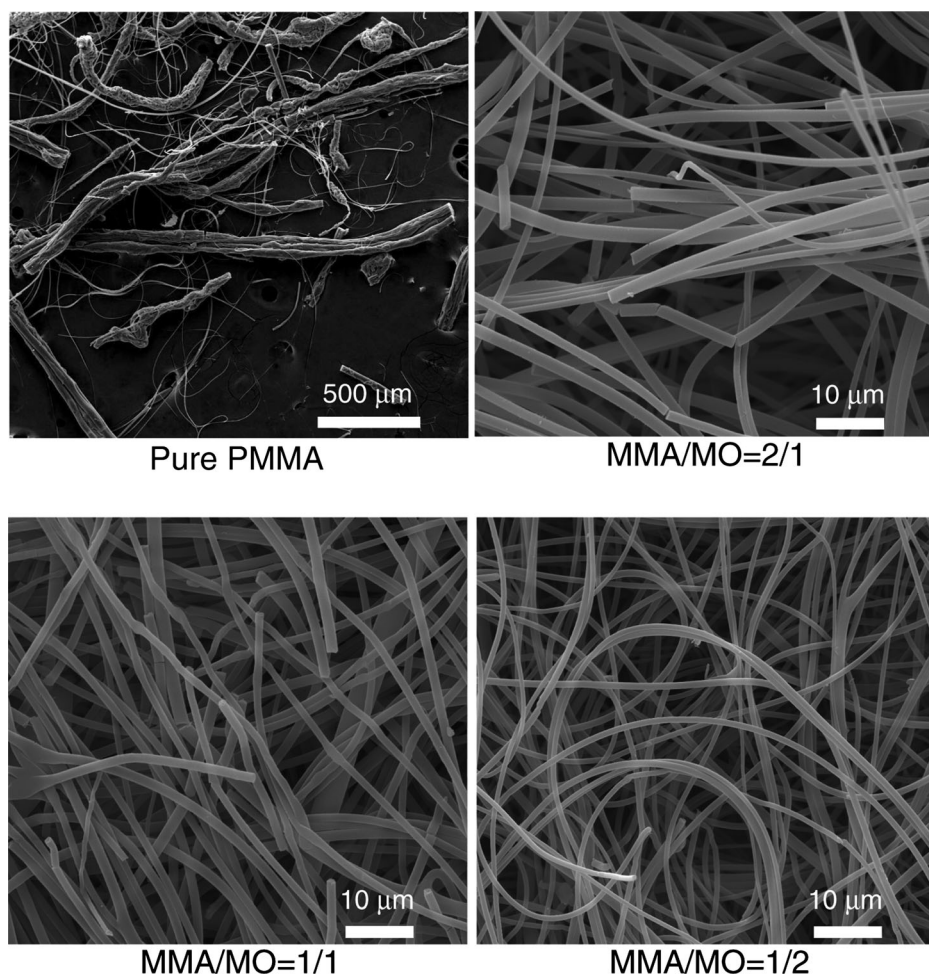


Figure 4.

SEM micrographs of the electrospun fibers of pure PMMA and MO/PVP complexes mixed with various fractions of PMMA. Note that the length scale for pure PMMA is much larger than for the MO/PVP complexes.

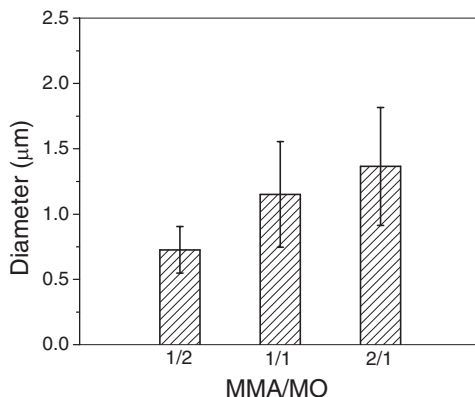


Figure 5.

Average diameter of the fibers for the different MMA/MO weight ratios investigated. The error bars show the standard deviation for at least 100 measurements.

higher conductivity and lower viscosity of the solutions with a larger fraction of polyelectrolyte. By comparison, very thick (over 5 μm) fibers are obtained from solutions of pure PMMA (15 wt %) in DMF (Figure 4).

The fibers were further investigated by differential scanning calorimetry to determine if phase separation occurred during the electrospinning process. Figure 6 shows the DSC scans up to 140 °C, below the T_g of the pure MO/PVP complex determined previously to be 183 °C^[15] (limited because thermogravimetric analysis of PMMA appeared to show the first traces of thermal

degradation near 140 °C). The data nevertheless allow the observation of clear phase separation in the mixed fibers since they all present a T_g at ~126 °C, close to that of pure PMMA at 121 °C. Assuming Fox-like behavior, this 5 °C increase of the T_g suggests that the PMMA-rich phase includes approximately 10% of the complex.

X-ray diffraction measurements were conducted to verify if the liquid crystalline order of MO/PVP is preserved in the fibers. Figure 7 compares the diffractograms of the fibers to those of the starting materials in powder form. Except for pure PMMA, all

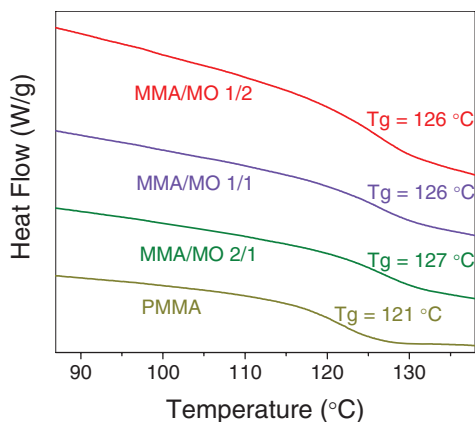


Figure 6.

DSC thermograms (3rd heating scan) of the electrospun fibers.

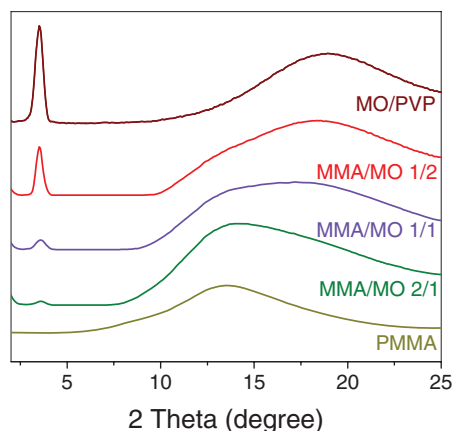


Figure 7.

X-ray diffractograms of the electrospun fibers with the different MMA/MO weight ratios investigated and of the pure compounds in powder form.

show the presence of a diffraction peak at small angles (ca. 3.55°) that corresponds to a *d* spacing of 2.5 nm, accompanied by a wide angle scattering halo centered at $2\theta \approx 19^\circ$. This shows that the smectic A liquid crystalline mesophase of MO/PVP^[14] is maintained in the electrospun fibers. Pure PMMA only presents a broad halo centered at 13° that partly overlaps the halo originating from the complex. With increasing addition of PMMA, the relative intensity of the small angle diffraction peak, in comparison to that of the wide-angle halo of the complex (as indicated by approximate curve fitting of the diffraction profiles), gradually decreases. This

decreasing tendency of the MO/PVP complex to form a liquid crystalline phase may be due in part to partial miscibility with PMMA, but is probably mainly due to kinetically limited mesophase formation. Indeed, the solvent evaporation is extremely rapid and occurs on a millisecond time scale during the electrospinning process. This often leads to metastable or out-of-equilibrium structures in electrospun nanofibers, which could also hinder mesophase formation. It is noteworthy that the 2D XRD patterns did not reveal any orientation of the liquid crystalline structure (not shown). Although this might indicate that there is no long-range orientation of the smectic A domains of the complex relative to the fiber axis (and therefore would not account for the anisotropic birefringence observed in Figure 3), it might also be due to the imperfect macroscopic alignment of the fibers within the bundles. It may be added that no long-range order was reported within the liquid crystalline domains of a block copolymer of poly(styrene-*b*-4-vinyl pyridine) hydrogen-bonded with equimolar pentadecylphenol.^[27,28]

Figure 8 shows longitudinal and cross-sectional TEM images of microtomed MMA/MO 1/2 fibers. A longitudinal structure consisting of alternating dark and bright strips can be observed. Since the fibers were stained with $K_2Cr_2O_7$, the dark sections should be due to the MO/PVP

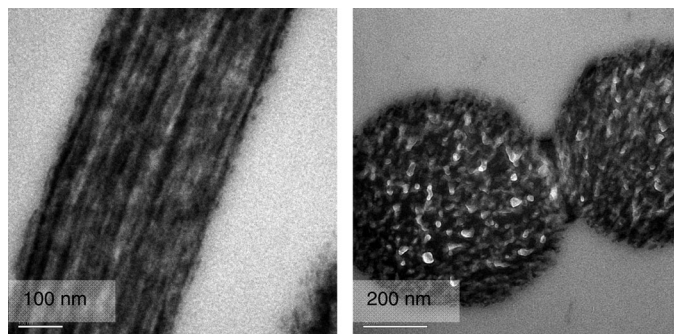


Figure 8.

TEM micrographs of the MMA/MO 1/2 fiber from longitudinal (left) and transversal (right) sections.

complex and the bright ones to the PMMA-rich phase. Irregular dark and white domains are also visible in the fiber cross-section (Figure 8, right), confirming that phase separation takes place all within the entire fiber. This phase-separated anisotropic structure consisting of phases with different refractive indices is likely to lead to “form birefringence”,^[26] and could partly explain the high birefringence observed by polarizing optical microscopy (Figure 3). We recently demonstrated that polarized Raman spectroscopy can be used to determine the level of molecular orientation in individual electrospun nanofibers, avoiding the need for well-aligned bundles as in the XRD experiments.^[29] In the next phase of this project, this technique will be applied to enable observation of both the initial orientation level and the impact of laser irradiation on the orientation of the methyl orange and the polymer within the electrospun fibers.

Conclusion

Nanophase-separated fibers were prepared by electrospinning of solutions of an azo-containing ionically-bonded liquid crystalline complex mixed with PMMA. The average diameter of the smooth and beadless fibers varies from 700 nm to 1.5 μm , increasing with PMMA fraction. DSC and TEM showed that the phase-separated morphology appears to be in the form of nanostrips tending to be oriented along the fiber axis. XRD showed that the complex maintains the smectic A liquid crystalline mesophase of the bulk complex, although its formation is partially hindered, probably due to partial miscibility with PMMA (about 10% in the PMMA-rich phase, as indicated by DSC) and/or for kinetic reasons. No orientation relative to the fiber axis within the liquid crystalline complex phase could be detected by 2D XRD. However, the fibers show significant birefringence by polarizing optical microscopy, ascribed mainly to form birefringence. The fibers prepared in

this report pave the way for the investigation of light-responsive behavior in these materials. Future work will focus on determining the orientation of all components in the initial fibers as well as in response to photo-induced orientation and on investigating photomechanical properties of the fibers, such as their photo-regulated shrinkage, stretching or other motion.

Acknowledgements: This work was supported by the Natural Sciences and Engineering Research Council of Canada (NSERC) and Fonds de recherche du Québec – Nature et Technologie (FRQNT). X.W. thanks the China Scholarship Council (CSC) and Université de Montréal for their financial support.

- [1] A. Greiner, J. H. Wendorff, *Angew. Chem. Int. Ed.* **2007**, 46, 5670.
- [2] Z.-M. Huang, Y. Z. Zhang, M. Kotaki, S. Ramakrishna, *Compos. Sci. Technol.* **2003**, 63, 2223.
- [3] J. D. Schiffman, C. L. Schauer, *Polymer Reviews* **2008**, 48, 317.
- [4] W. E. Teo, S. Ramakrishna, *Nanotechnology* **2006**, 17, R89.
- [5] Y. Liu, C. Pellerin, *Polymer* **2009**, 50, 2601.
- [6] Y. Liu, H. Antaya, C. Pellerin, *J. Phys. Chem. B* **2010**, 114, 2373.
- [7] T. Uyar, P. Kingshott, F. Besenbacher, *Angew. Chem. Int. Ed.* **2008**, 47, 9108.
- [8] T. Uyar, Y. Nur, J. Hacıoglu, F. Besenbacher, *Nanotechnology* **2009**, 20, 125703.
- [9] C. Subramanian, R. A. Weiss, M. T. Shaw, *Polymer* **2010**, 51, 1983.
- [10] H. Rau, “Photoisomerization of azobenzenes”. in: *Photochemistry and Photophysics*, J. K. Rabek, (Ed., CRC Press, Boca Raton, FL **1990**, p. 119.
- [11] A. Natansohn, P. Rochon, *Chem. Rev.* **2002**, 102, 4139.
- [12] M. Yamada, M. Kondo, J.-i. Mamiya, Y. Yu, M. Kinoshita, C. J. Barrett, T. Ikeda, *Angew. Chem. Int. Ed.* **2008**, 47, 4986.
- [13] T. Ikeda, J.-i. Mamiya, Y. Yu, *Angew. Chem. Int. Ed.* **2007**, 46, 506.
- [14] Q. Zhang, C. G. Bazuin, C. J. Barrett, *Chem. Mater.* **2008**, 20, 29.
- [15] Q. Zhang, X. Wang, C. J. Barrett, C. G. Bazuin, *Chem. Mater.* **2009**, 21, 3216.
- [16] E. Merian, *Textile Research Journal* **1966**, 36, 612.
- [17] C. L. Jackson, M. T. Shaw, *Int. Mater. Rev.* **1991**, 36, 165.
- [18] S. Krause, R. Dersch, J. H. Wendorff, H. Finkelmann, *Macromol. Rapid Commun.* **2007**, 28, 2062.

- [19] K. Nakashima, K. Tsuboi, H. Matsumoto, R. Ishige, M. Tokita, J. Watanabe, A. Tanioka, *Macromol. Rapid Commun.* **2010**, 31, 1641.
- [20] Y. Wu, Q. An, J. Yin, T. Hua, H. Xie, G. Li, H. Tang, *Colloid. Polym. Sci.* **2008**, 286, 897.
- [21] H. Nie, A. He, J. Zheng, S. Xu, J. Li, C. C. Han, *Biomacromolecules* **2008**, 9, 1362.
- [22] H. Chen, J. D. Snyder, Y. A. Elabd, *Macromolecules* **2008**, 41, 128.
- [23] M. G. McKee, M. T. Hunley, J. M. Layman, T. E. Long, *Macromolecules* **2006**, 39, 575.
- [24] P. Gupta, C. Elkins, T. E. Long, G. L. Wilkes, *Polymer* **2005**, 46, 4799.
- [25] S. Piperno, L. Lozzi, R. Rastelli, M. Passacantando, S. Santucci, *Appl. Surf. Sci.* **2006**, 252, 5583.
- [26] I. M. Ward, “*Structure and Properties of Oriented Polymers*”, 2nd edition Chapman & Hall, New York **1997**.
- [27] T. Ruotsalainen, J. Turku, P. Heikkilä, J. Ruokolainen, A. Nykanen, T. Laitinen, M. Torkkeli, R. Serimaa, G. ten Brinke, A. Harlin, O. Ikkala, *Adv. Mater.* **2005**, 17, 1048.
- [28] T. Ruotsalainen, J. Turku, P. Hiekkataipale, U. Vainio, R. Serimaa, G. ten Brinke, A. Harlin, J. Ruokolainen, O. Ikkala, *Soft Matter* **2007**, 3, 978.
- [29] M. Richard-Lacroix, C. Pellerin, *Macromolecules* **2012**, 45, 1946.